

Supporting Information

Giant Piezomagnetism in Mn_3NiN

David Boldrin^{1‡}, Andrei P. Mihai^{2‡}, Bin Zou^{2‡}, Jan Zemen^{1,3}, Ryan Thompson¹, Ecaterina Ware², Bogdan V. Neamtu⁴, Luis Ghivelder⁵, Bryan Esser⁶, David W. McComb⁶, Peter Petrov² and Lesley F. Cohen¹*

1. Department of Physics, Blackett Laboratory, Imperial College London, London SW7 2AZ, United Kingdom

2. Department of Materials, Imperial College London, London SW7 2BP, United Kingdom

3. Faculty of Electrical Engineering, Czech Technical University in Prague, Technická 2, Prague 166 27, Czech Republic

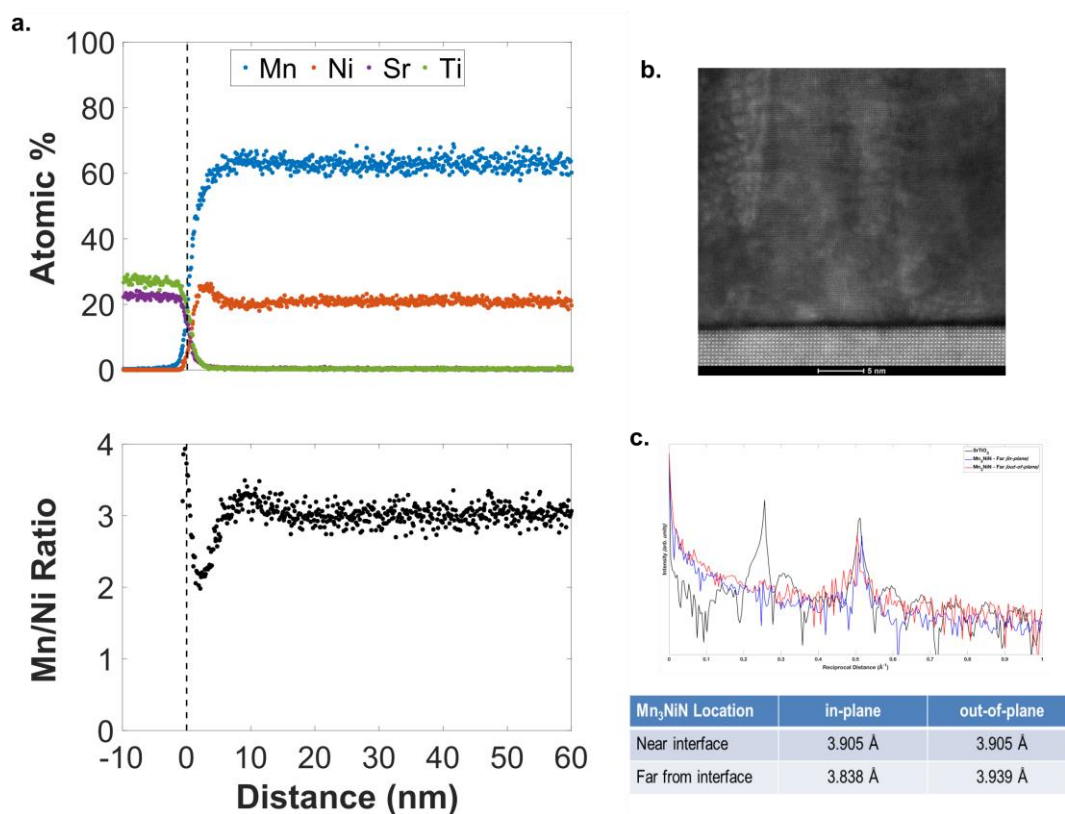
4. Material Science and Technology Department, Technical University of Cluj-Napoca, 103-105 Muncii, Romania

5. Instituto de Fisica, Universidade Federal do Rio de Janeiro, 21941-972 Rio de Janeiro, RJ, Brazil

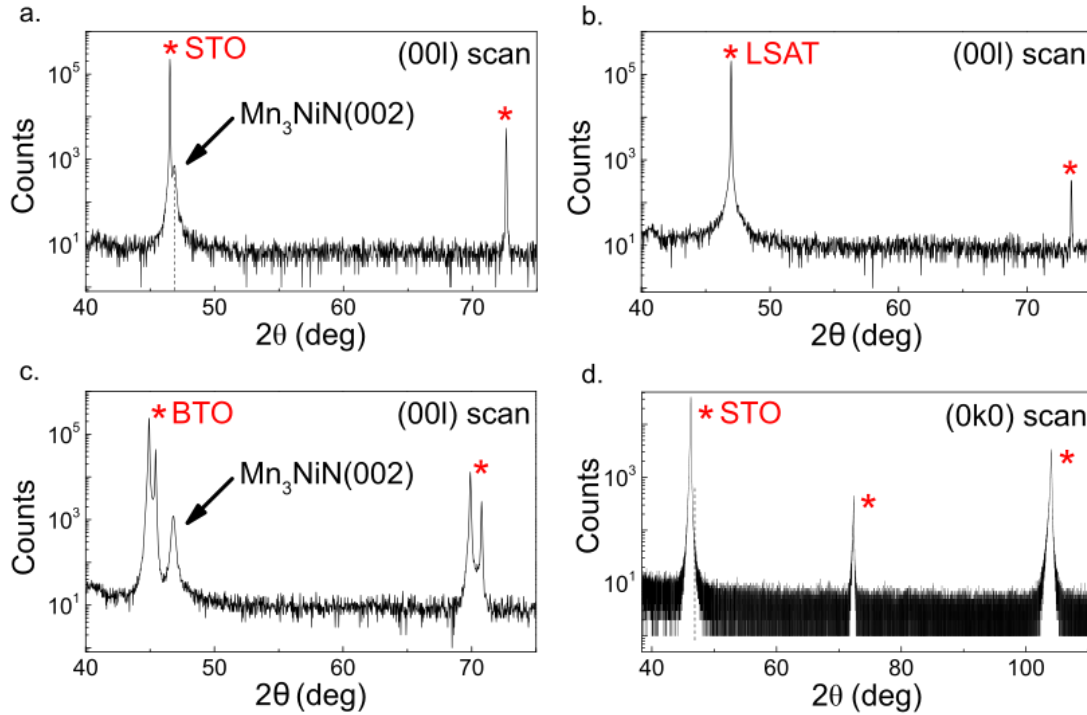
6. Center for Electron Microscopy and Analysis, 1305 Kinnear Road, Columbus, OH 43212, United States of America

Corresponding Author

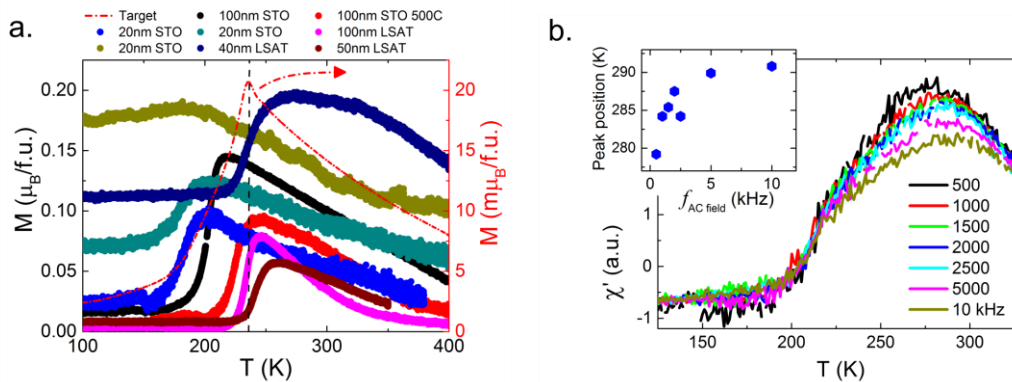
*David Boldrin, d.boldrin@imperial.ac.uk



Supplementary Figure S1. (a) EDX profile on Mn₃NiN(100)/STO taken using a Titan HAADF-STEM. ** Interface locations were determined by the location of the inflection point in the Sr signal (net counts) under the assumption that Mn cannot substitute onto the A sites of STO. (b) HAADF-STEM image of STO/Mn₃NiN(100) showing the epitaxial registration between the STO substrate and the Mn₃NiN thin film. The mottle contrast is most likely due to oxidation of the free surfaces created after milling, the 2nm dark band at the interface is due to a Mn poor, Ni rich layer. (c) Fourier transform of the STEM image 30nm from the interface. The table shows the in-plane and out-of-plane lattice parameters ~2nm and ~30nm from the interface. The Poisson ratio far from the interface is $\nu = 0.41$.



Supplementary Figure S2: (00l) X-ray diffraction scans on 100nm Mn₃NiN films grown on (a) STO, (b) LSAT and (c) BTO; (d) (0k0) X-ray diffraction scan of a 300nm thick Mn₃NiN film, showing that even for thick films the Mn₃NiN peak cannot be distinguished from the substrate.



Supplementary Figure S3. (a) Magnetisation measurements as a function of temperature of various Mn₃NiN thin films with different thicknesses grown on STO and LSAT substrates at 400°C and 500°C, respectively, unless stated otherwise in the legend, and under 5 mTorr nitrogen partial pressure. All data were collected on warming in an applied field of 0.05T after being cooled in zero field. Vertical line shows the Neel temperature of the bulk sample. (b) AC susceptibility data collected on a STO/Mn₃NiN(100nm) thin film.

Sample	Deposition temperature (°C)	Mn (at%)	Ni (at%)	Mn/Ni ratio	XRD c (Å)	Calculated a (Å)	$\epsilon_{xx} = \epsilon_{yy}$ (%)	TEM c (Å)	TEM a (Å)	ν
STO 100nm a (302)	500	59(1)	22(1)	2.75	3.8787	3.8812	0.02	3.939	3.838	0.41
STO 100nm b (308)	400	58(1)	19.8(5)	2.93	3.8977	3.8735	-0.18			
STO 20nm (404)	400	58(2)	22(1)	3	3.9045	3.8707	-0.25			
LSAT 40nm (419)	500	64(2)	21(1)	3	3.8680	3.8856	0.13			
BTO 100nm (471)	500	57(2)	25(2)	2.6	3.8857	3.8784	-0.05			
LSAT 50nm (388)	500	-	-	-	3.8654	3.8867	0.16			
LSAT 100nm (470)	500	-	-	-	3.8657	3.8866	0.16			
STO 20nm (434)	400	-	-	-	3.9009	3.8721	-0.22			
STO 20nm (501)	400	-	-	-	3.9045	3.8707	-0.25			

Supplementary Table S1. Collated EDX, X-ray diffraction and TEM results for Mn₃NiN thin films on STO, BTO and LSAT substrates. The a lattice parameter is calculated from the c lattice parameter determined from XRD and the measured Poisson ratio $\nu = 0.41$.